

# Rhodium-Catalyzed C–H Activation of Phenacyl Ammonium Salts Assisted by an Oxidizing C–N Bond: A Combination of Experimental and Theoretical Studies

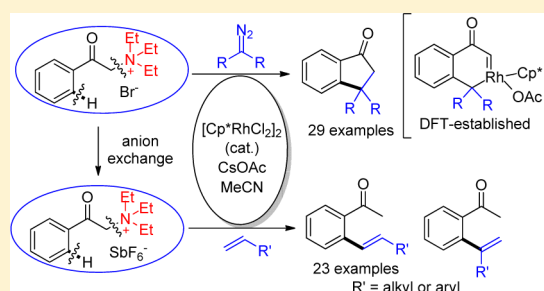
Songjie Yu,<sup>†</sup> Song Liu,<sup>‡</sup> Yu Lan,<sup>\*,‡</sup> Boshun Wan,<sup>\*,†</sup> and Xingwei Li<sup>\*,†</sup>

<sup>†</sup>Dalian Institute of Chemical Physics, Chinese Academy of Sciences, Dalian 116023, China

<sup>‡</sup>School of Chemistry and Chemical Engineering, Chongqing University, Chongqing 400030, China

**S** Supporting Information

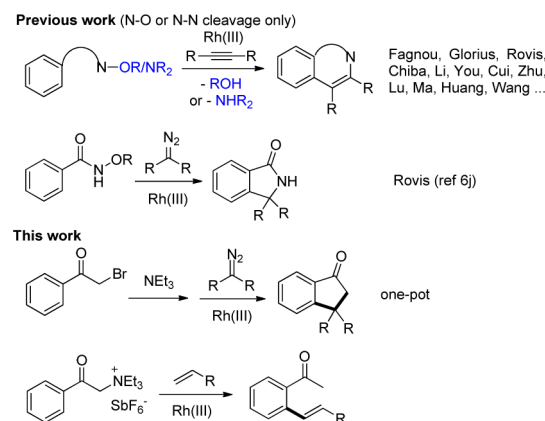
**ABSTRACT:** Rh(III)-catalyzed C–H activation assisted by an oxidizing directing group has evolved to a mild and redox-economic strategy for the construction of heterocycles. Despite the success, these coupling systems are currently limited to cleavage of an oxidizing N–O or N–N bond. Cleavage of an oxidizing C–N bond, which allows for complementary carbocycle synthesis, is unprecedented. In this article,  $\alpha$ -ammonium acetophenones with an oxidizing C–N bond have been designed as substrates for Rh(III)-catalyzed C–H activation under redox-neutral conditions. The coupling with  $\alpha$ -diazo esters afforded benzocyclopentanones, and the coupling with unactivated alkenes such as styrenes and aliphatic olefins gave *ortho*-olefinated acetophenones. In both systems the reactions proceeded with a broad scope, high efficiency, and functional group tolerance. Moreover, efficient one-pot coupling of diazo esters has been realized starting from  $\alpha$ -bromoacetophenones and triethylamine. The reaction mechanism for the coupling with diazo esters has been studied by a combination of experimental and theoretical methods. In particular, three distinct mechanistic pathways have been scrutinized by DFT studies, which revealed that the C–H activation occurs via a C-bound enolate-assisted concerted metalation–deprotonation mechanism and is rate-limiting. In subsequent C–C formation steps, the lowest energy pathway involves two rhodium carbene species as key intermediates.



## INTRODUCTION

Recently, C–H functionalization has been extensively explored as a versatile and highly efficient strategy for the synthesis of important skeletons implicated in organics, natural products, and pharmaceutical molecules.<sup>1,2</sup> Along with the extensively studied rhodium(III)-catalyzed functionalization of C–H bonds with alkynes,<sup>3</sup> alkenes,<sup>4</sup> and other unsaturated molecules<sup>5</sup> in the presence of an external oxidant, the coupling system has been extended to internal oxidants based on cleavage of polar N–O and N–N bonds in oxidizing directing groups (DGs) (Scheme 1).<sup>6</sup> These systems have the advantage of redox-economy in that no external oxidant is necessary. Thus, building on the seminal strategy of using an internally oxidizing N–O DG pioneered by Fagnou<sup>7</sup> and Glorius,<sup>8</sup> a number of Rh(III)-catalyzed C–H activation systems were developed by taking advantage of oxidizing potential of N–O and N–N bonds in oximes,<sup>9</sup> *N*-pivaloxybenzamide,<sup>6</sup> hydrazines,<sup>10</sup> phenoxyamides,<sup>11</sup> *N*-oxides,<sup>12</sup> and others.<sup>13</sup> These systems typically involve alkynes and alkenes as a coupling partner, resulting in heterocycle synthesis. On the other hand, cleavage of a polar C–N bond in redox-neutral C–H activation is unprecedented because of the low reactivity.<sup>14</sup> However, this is of great significance because it may allow the efficient construction of complementary carbocycles.

## Scheme 1. Rh(III)-Catalyzed C–H Activation Assisted by Oxidizing Directing Groups



While the oxidizing DG strategy is a rising concept in C–H activation/cross-couplings and it favorably allows for milder conditions and high selectivity, it requires the prior preparation of the substrate. Therefore, this strategy is of high synthetic value when the substrates are readily synthesized and are cost-

Received: November 17, 2014

Published: January 8, 2015

effective, especially when the alternative C–H activation using external oxidants is not applicable or is only poorly applicable.

With these criteria in mind, we pondered the feasibility of using a readily available  $\alpha$ -heteroatom-substituted acetophenone (ideally  $\alpha$ -haloacetophenone) as an arene substrate for C–H activation in the context of redox-neutral couplings. However, the following challenges have to be solved:

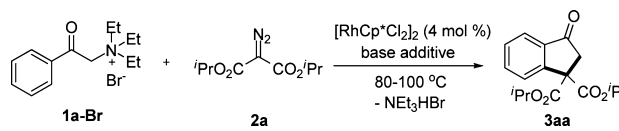
- (1)  $\alpha$ -Heteroatom-substituted acetophenones contain an electrophilic carbonyl group, and, with enhanced acidity of the methylene protons, the methylene can be both an electrophilic and a nucleophilic site. Consequently, low stability and self-condensation may pose selectivity issues.
- (2) The C–H activation and the subsequent carbon–heteroatom cleavage need to be compatible. In addition, the leaving group should not inhibit the Rh(III) catalyst.
- (3) The ligating ability of a ketone carbonyl is generally low,<sup>4b,15</sup> and its directing effect needs to be enhanced, possibly by proper installation of an  $\alpha$ -substituent.

**Substrate Design.** It seems that it all boils down to proper design of a cleavable and reactive carbon–heteroatom bond. Glorius and co-workers recently reported Rh-catalyzed coupling involving phenacyl tosylates;<sup>16</sup> however, they reacted as an electrophilic coupling partner rather than as an arene source. Thus, no redox-neutral C–H activation of  $\alpha$ -(pseudo)-haloacetophenones has been reported, although the C–H activation of PhC(O)CH<sub>2</sub>CN resulting in CN-retentive oxidative coupling with alkynes has been realized.<sup>17</sup> While they seem readily available as an arene source for such a purpose,  $\alpha$ -chloro- or bromoacetophenones all failed to couple with alkenes and alkynes under various rhodium- and ruthenium-catalyzed conditions, likely due to the aforementioned challenges. We reasoned that simple quaternization with a tertiary amine may provide an ionic substrate that can satisfy the criteria of substrate design (Scheme 1, bottom). This is because the electron-withdrawing quaternary ammonium group enhances the acidity at the  $\alpha$  position, leading to facile formation of an enolate complex. In addition, a non-inhibiting protic ammonium salt may be generated as a co-product. Thus, the introduction of an  $\alpha$ -ammonium moiety may serve to activate the substrate. We now report our design of the first internally oxidizing C–N DG in rhodium-catalyzed C–H activation/coupling with diazoesters<sup>18</sup> and unactivated alkenes.

## RESULTS AND DISCUSSION

**Optimization Studies.** The designed phenacyltriethylammonium bromide (**1a-Br**) was readily obtained in nearly quantitative yield from the room temperature reaction between  $\alpha$ -bromoacetophenone and NEt<sub>3</sub>. We then screened the reaction conditions for the coupling of **1a-Br** with di-isopropyl diazomalonate (**2a**). It was found that the desired coupling did occur to variable extents in different solvents when catalyzed by [Cp\*RhCl<sub>2</sub>]<sub>2</sub> (4 mol %) in the presence of CsOAc (2.0 equiv) (Table 1). A rather low yield of benzocyclopentanone **3aa** was isolated when a less polar solvent such as DCM, DCE, or THF was employed (entries 1, 2, 4). The gas chromatography (GC) yield was improved to 74% when acetone was used as a solvent (entry 3), and gratifyingly **3aa** was isolated in 93% yield when MeCN was selected as the solvent (entry 5). CsOAc proved to be the optimal base; switching to other bases such as CsOPiv or NaOAc led to a slightly or significantly lower coupling efficiency (entries 6, 7). Variation of the amount of the base

**Table 1. Optimization of Reaction Conditions<sup>a</sup>**



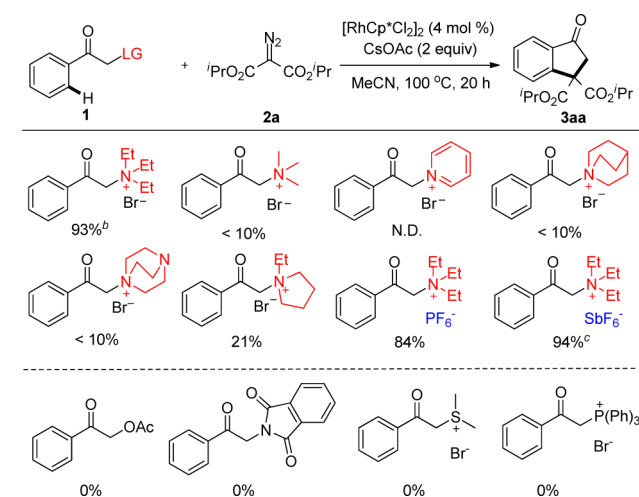
entry	base (equiv)	solvent	temp, °C	yield, <sup>b</sup> %
1	CsOAc (2.0)	DCM	100	23
2	CsOAc (2.0)	DCE	100	nd
3	CsOAc (2.0)	acetone	100	74
4	CsOAc (2.0)	THF	100	<10
5	CsOAc (2.0)	MeCN	100	93 <sup>c</sup>
6	NaOAc (2.0)	MeCN	100	<10
7	CsOPiv (2.0)	MeCN	100	89
8	CsOAc (2.0)	MeCN	80	85
9	CsOAc (0.3)	MeCN	100	80
10	–	MeCN	100	nd
11 <sup>d</sup>	CsOAc (2.0)	MeCN	100	nd

<sup>a</sup>Reaction conditions: **1a-Br** (0.24 mmol), **2a** (0.2 mmol), solvent (3 mL), 100 °C, 20 h, under N<sub>2</sub> in a sealed tube. <sup>b</sup>GC yield using biphenyl as an internal standard. nd = not determined. <sup>c</sup>Isolated yield. <sup>d</sup>No catalyst was used.

revealed that the product was obtained in lower yield when the amount of CsOAc was reduced to 0.3 equiv (entry 9). In addition, no free NEt<sub>3</sub> was detected by GC-MS analysis of a crude product, so triethylammonium bromide or acetate should be a co-product.

**Effects of Other Leaving Groups and Anions.** Other parameters in the coupling of different phenacyl quaternary ammonium salts were further examined under the optimized conditions (Scheme 2). It turned out that ammoniums derived

**Scheme 2. Effects of Other Reaction Parameters<sup>a</sup>**



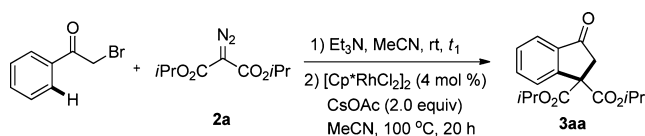
<sup>a</sup>See Table 1, entry 5 for reaction conditions; GC yield using biphenyl as an internal standard. <sup>b</sup>Yield of the isolated product. <sup>c</sup>[Cp\*Rh(MeCN)<sub>3</sub>][SbF<sub>6</sub>]<sub>2</sub> (8 mol %) was used as a catalyst in DCE (3 mL).

from other tertiary amines including NMe<sub>3</sub>, pyridine, and DABCO all failed to give efficient or any coupling. This indicates that the coupling was strongly affected by a combination of electronic and steric effects of the tertiary amine unit. When the triethylammonium unit was fixed, variation of the anion to PF<sub>6</sub><sup>–</sup> and SbF<sub>6</sub><sup>–</sup> resulted in marginal influence, as in the isolation of **3aa** in consistently high yield.

These results tend to suggest that the coordinating ability of the anion is of minimal significance. In addition, limited influence on the isolated yield was also observed when an extra amount of  $\text{NEt}_3$  (1 equiv) was introduced to the standard conditions, under which **3aa** was still isolated in 83% yield. Extensive screening revealed that the ammonium moiety proved necessary because using acetophenones bearing other  $\alpha$  leaving groups such as acetate, phthalimide, dimethylsulfide, and triphenylphosphine all failed to give any desired product (Scheme 2). These outcomes highlighted the significant role of the ammonium group.

**The One-Pot Conditions.** The tolerance of  $\text{NEt}_3$  in this reaction bodes well for a one-pot reaction. However, coupling using a premixed  $\text{PhC(O)CH}_2\text{Br}$ ,  $\text{NEt}_3$ , the rhodium catalyst, diazo ester **2a**, and  $\text{CsOAc}$  in  $\text{MeCN}$  gave **3aa** only in poor yield (Table 2). Importantly, pre-stirring of  $\text{PhC(O)CH}_2\text{Br}$  and

Table 2. One-Pot Conditions and a Gram-Scale Reaction<sup>a</sup>



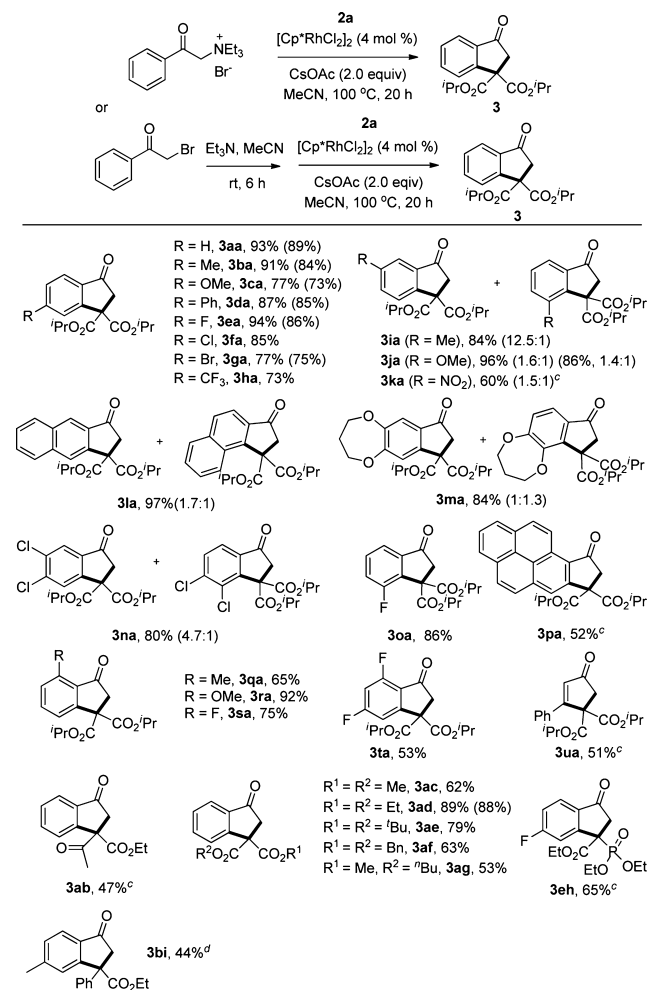
reactants, mmol		2a	$t_1$	yield, <sup>b</sup> %
$\text{PhC(O)CH}_2\text{Br}$	$\text{NEt}_3$			
0.24	0	0.2	0	<10
0.24	0.3	0.2	10 min	30
0.24	0.3	0.2	6.0 h	89
6.0	7.5	5.0	7.0 h	78 <sup>c</sup>

<sup>a</sup>Reaction conditions: bromoacetophenone and  $\text{NEt}_3$  were stirred in  $\text{MeCN}$  (0.1 M) at room temperature for the indicated time.  $[\text{Cp}^*\text{RhCl}_2]_2$ ,  $\text{CsOAc}$ , and **2a** were then added and stirred at  $100^\circ\text{C}$  for 20 h under  $\text{N}_2$  in a sealed tube. <sup>b</sup>Isolated yield. <sup>c</sup>2 mol % of  $[\text{Cp}^*\text{RhCl}_2]_2$  was used.

$\text{NEt}_3$  in  $\text{MeCN}$  for 6 h led to in situ generation of the substrate **1a-Br**. Subsequent addition of the rhodium catalyst and other reagents allowed the reaction to proceed smoothly under the standard conditions, from which product **3aa** was isolated in 89% yield (Table 2). Furthermore, the one-pot reaction was successfully extended to a gram-scale synthesis of **3aa** (5 mmol of **2a**), where using 2 mol % of the catalyst, the product was still isolated in 78% yield (1.19 g).

**Substrate Scope.** By following the single-step and the one-pot conditions, the scope of this reaction was next explored (Scheme 3). Phenacyl ammoniums prepared beforehand bearing various electron-donating, electron-withdrawing, and halide substituents at the *para* positions all underwent smooth coupling with diazomalonnate **2a**, and the cyclization products were isolated in 73–91% yields. Introduction of a methyl, fluoro, or methoxy group to the *ortho* position of the benzene ring is fully tolerated, indicative of compatibility of the steric effect. Various *meta*-substituted substrates also coupled efficiently, and in most cases C–H activation occurred at both positions with low to moderate regioselectivities (1.3–12.5:1), and the two regioisomeric products could be chromatographically separated. Of note, a *meta*-nitro group, which is often problematic in C–H activation systems,<sup>19</sup> is fully compatible. An exception in selectivity was found for a *meta*-fluoro-substituted substrate, where C–H functionalization occurred selectively at the more hindered position (**3oa**).<sup>20</sup> Moreover, one-pot reactions starting from  $\alpha$ -bromoaceto-

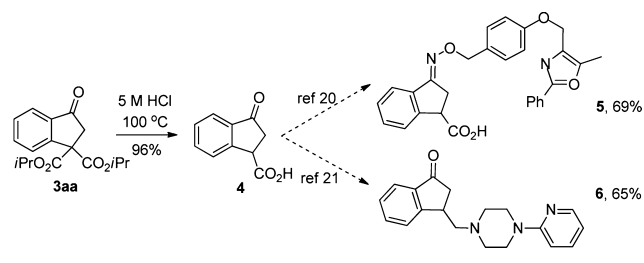
Scheme 3. Coupling with  $\alpha$ -Diazooesters<sup>a</sup>



phenones afforded consistently high yields (**3aa**, **3ba**, **3ca**, **3da**, **3ea**, **3ga**, **3ja**, and **3ad**), and they are only slightly lower than those using the corresponding phenacyl ammonium bromides prepared beforehand. This C–H activation reaction is not limited to an arene substrate, and an olefinic substrate also reacted under our modified conditions to afford a cyclopentenone (**3ua**) in moderate yield. The scope of diazo coupling partners has also been established, and a wide scope of symmetric and non-symmetric  $\alpha$ -diazomalonnates,  $\alpha$ -diazooacetates (**3ab**), and  $\alpha$ -diazophosphates (**3eh**) all coupled smoothly in moderate to high yields (47–89%). Importantly, a push–pull diazoester also coupled to give **3bi** with a quaternary chiral center, albeit in lower yield (44%).

**Functionalization of a Product.** The coupled product **3aa** was readily functionalized upon hydrolysis in aqueous  $\text{HCl}$  to give carboxylic acid **4** in 96% yield (Scheme 4). Acid **4** has been reported to serve as a direct precursor to several important

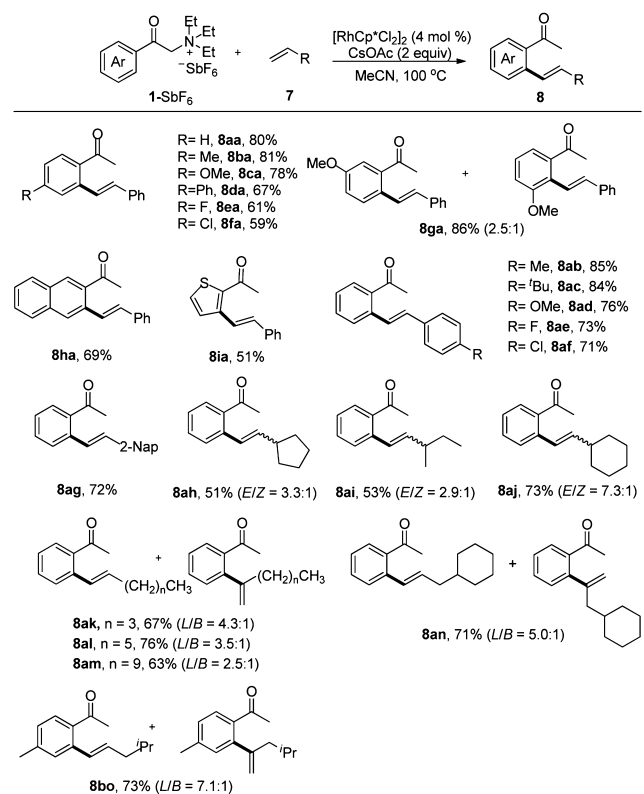
Scheme 4. Functionalization of Product 3aa



heterocyclic pharmaceuticals (**5**<sup>21</sup> and **6**<sup>22</sup>) that are known to exhibit biological activities.

**Coupling with Olefins.** We next extended the coupling partner to styrenes. Our extensive screening (see the Supporting Information (SI)) revealed that the bromide salt **1a-Br** coupled with styrene only in poor efficiency under various conditions, likely due to the inhibition of the bromide anion. Indeed, under the conditions that are optimal for the coupling with diazo esters, switching to the hexafluoroantimonate salt (**1a-SbF<sub>6</sub>**) afforded an *ortho*-olefinated acetophenone **8aa** in high yield (see SI). This may suggest that a similar mechanism is operational (see SI for a proposed catalytic cycle).

The substrate scope of this olefination reaction is also broad (Scheme 5). Thus, *o*-styrylacetophenones were isolated in moderate to good yields from the coupling of various quaternary ammonium salts with styrenes (**8aa–8ha**). While both regioisomers were also generated for a *meta*-substituted

Scheme 5. Coupling with Olefins<sup>a,b</sup>

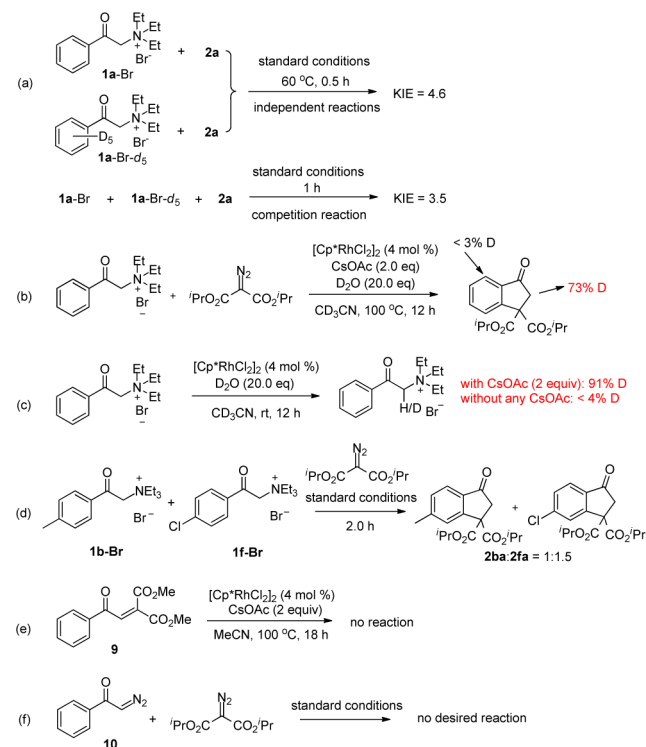
<sup>a</sup>Reaction conditions: **1-SbF<sub>6</sub>** (0.24 mmol), olefin **7** (0.2 mmol), [Cp\***RhCl<sub>2</sub>**]<sub>2</sub> (4 mol %), CsOAc (0.4 mmol), MeCN (3 mL), 100 °C, 20 h, under N<sub>2</sub> in a sealed tube. <sup>b</sup>Isolated yield.

arene, the reaction is more selective and the major product corresponds to C–H activation at the less hindered *ortho* site (**8ga**, **8ha**). Furthermore, the arene ring is not limited to benzene, as in the isolation of a 3-olefinated thiophene **8ia** in moderate yield. Styrenes bearing different electron-donating and withdrawing groups (**8ab–8ag**) were fully compatible. Further extension to less reactive aliphatic olefins<sup>8,23</sup> also proved successful. However, the coupling with these olefins followed olefin-dependent selectivity in overall moderate to good yields. Thus, coupling with an  $\alpha$ -branched olefin occurred at the terminal position to afford two stereoisomeric products (**8ah–8aj**) in an *E/Z* ratio ranging from 2.9:1 to 7.3:1. In contrast, the coupling with a primary alkyl olefin consistently occurred at both the terminal and internal positions (**8ak–8bo**) and afforded a mixture of the 1,2-disubstituted *E*-olefin (major) and the 1,1-disubstituted olefin (minor), while the 1,2-disubstituted *Z*-olefin was essentially not observed (<5%). To our surprise, no desired coupling occurred when acrylate esters were applied, and this is in sharp contrast to their typically high reactivity. These results clearly demonstrated the significant electronic and steric effects of the olefin substrate. We noted that although Glorius and co-workers have recently reported the Rh(III)-catalyzed *ortho* C–H olefination of acetophenones using an external oxidant,<sup>4b</sup> the olefin substrates were limited to styrenes and acrylates, and no reaction has been reported for aliphatic olefins. Thus, the current redox-neutral coupling system<sup>8,12,24</sup> can complement the existing methods.

## EXPERIMENTAL MECHANISTIC STUDIES

Some experiments have been performed to explore the mechanism (Scheme 6). To better understand the C–H activation process, kinetic isotope effect was measured from two side-by-side reactions using **1a-Br** and **1a-Br-d<sub>5</sub>** at a lower temperature (see Scheme 6a and the SI), and a *k<sub>H</sub>/k<sub>D</sub>* value of 4.6 was obtained. In addition, the competitive coupling of an equimolar mixture of **1a-Br** and **1a-Br-d<sub>5</sub>** with diazo

Scheme 6. Experimental Studies on the Mechanism

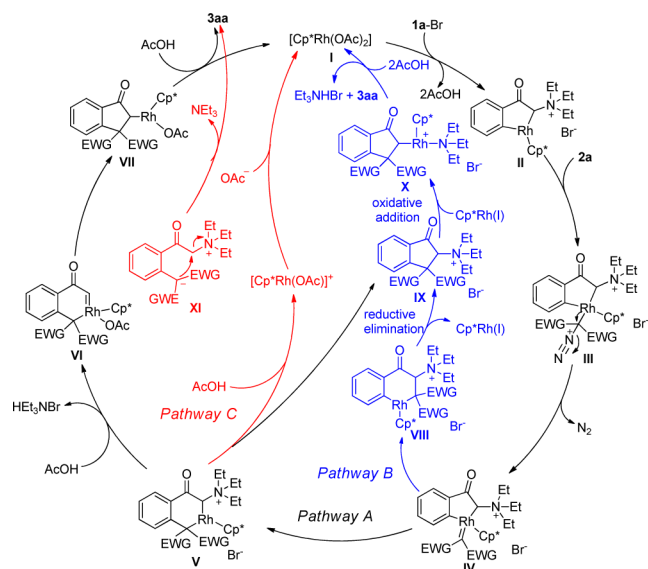




ester **2a** gave a consistent value of  $k_H/k_D = 3.5$  on the basis of  $^1\text{H}$  NMR analysis. These results suggested that C–H cleavage is likely involved in the rate-limiting step. Coupling of **1a-Br** and **2a** under the standard conditions in the presence of  $\text{D}_2\text{O}$  afforded **3aa-d<sub>n</sub>** with extensive H/D exchange (73% D) at the methylene position (Scheme 6b). However, no H/D exchange was detected at the *ortho* position of the product, indicative of the irreversibility of the C–H activation process under the catalytic conditions. Further control experiments revealed that the H/D exchange is ascribable to precoupling H/D exchange in the substrate (Scheme 6c). The H/D exchange in the substrate is also directly correlated to the  $\text{CsOAc}$  and it could occur even in the absence of the Rh(III) catalyst. Control experiments also showed that although a reaction using  $[\text{RhCp}^*(\text{OAc})_2]$  (6 mol %) as a catalyst in the absence of any  $\text{CsOAc}$  only afforded the product in low yield, **3aa** was isolated in 80% yield from the coupling of **1-SbF<sub>6</sub>** with **2a** when  $\text{CsOAc}$  (2.0 equiv) was introduced. Thus, deprotonation of the  $\alpha$  proton in the substrate plays an important role in catalysis. Indeed, a competitive coupling between two ammonium salts differing in electronic effects points to the conclusion that an electron-poor arene substrate tends to react at a higher rate (Scheme 6d). To further explore the reaction mechanism, a possible olefin intermediate **9** was prepared and was subjected to the standard conditions (Scheme 6e). No conversion was detected by GC-MS, and the starting material was fully recovered. Therefore, the possibility of initial olefination between **1a-Br** and dimethyl  $\alpha$ -diazomalonate followed by intramolecular insertion of the *ortho* C–H bond to the olefin can be ruled out. Furthermore, to probe if the reaction could be initiated by rhodium carbene formation followed by carbene-directed C–H activation, diazo compound **10**, a carbene precursor, was prepared and was subjected to the reaction conditions (Scheme 6f). No desired product was detected and only decomposition was observed. This observation suggests that it is unlikely that a carbene DG is formed first and it facilitates subsequent cyclometalation. We have extensively attempted but failed to isolate any cyclometalation intermediate under various stoichiometric reaction conditions, so it remains a question whether the reaction is initiated by C- or O-coordination of the enolate of **1a-Br**, which is to be best answered by DFT studies.

**Three Possible Mechanisms.** To gain mechanistic details of the coupling of phenacyl ammoniums with diazomalonates, three possible reaction pathways have been proposed starting from  $\text{RhCp}^*(\text{OAc})_2$  that proved to be an active catalyst (Scheme 7). These pathways were evaluated by theoretical studies at the DFT level. As given in Scheme

**Scheme 7. Three Possible Mechanistic Pathways for the Coupling of Phenacyl Ammonium Salts with a Diazomalonate**



7, C- or O-coordination of the enolate of **1a-Br** followed by cyclometalation affords a rhodacyclic intermediate **II** (shown for C-coordination only).<sup>25</sup> Subsequent coordination of the diazo substrate is followed by denitrogenation to generate a carbene species **IV** as a common intermediate.<sup>18a,26</sup> In pathway A (black), which involves the intermediacy of two carbene species, the subsequent migratory insertion of the Rh–Ar bond of **IV** into the carbene species generates a Rh(III) dialkyl intermediate **V**. This intermediate is then proposed to undergo  $\alpha$ -elimination of  $\text{NEt}_3$  to afford an  $\alpha$ -oxo carbenoid species **VI**.<sup>27</sup> Further migratory insertion of the Rh–alkyl bond of **VI** into the carbenoid gives an enolate intermediate **VII**. Protonolysis by  $\text{AcOH}$  furnishes the final product with the regeneration of the catalyst. In pathway B (blue), the carbene species **IV** may undergo insertion into the Rh–alkyl bond to lead to an intermediate **VIII** that is the isomer of **V**. This intermediate **VIII** is then proposed to undergo  $\text{C}(\text{sp}^2)\text{--}\text{C}(\text{sp}^3)$  reductive elimination to generate an  $\alpha$ -ammonium-functionalized benzocyclopentanone **IX** together with a Rh(I) species. The polar C–N bond in **IX** is proposed to oxidatively add back to the Rh(I) intermediate to give Rh(III) enolate **X**, protonolysis of which by  $\text{AcOH}$  furnishes the final product. The pathway C (red) overlaps with pathway A, but the dialkyl intermediate **V** undergoes protonolysis by  $\text{AcOH}$  to give a zwitterionic intermediate **XI**, which might undergo uncatalyzed, intermolecular  $\text{S}_{\text{N}}2$  substitution to furnish the same coupled product.

**Computational Methods.** All the DFT calculations were carried out using the GAUSSIAN 09 series of programs.<sup>28</sup> Density functional theory and B3LYP<sup>29</sup> with a standard 6-31+G(d) basis set (SDD basis set for Rh) was used for geometry optimizations. The solvent effects were considered by single-point calculations on the gas-phase stationary points with a SMD continuum solvation model.<sup>30</sup> The M06<sup>31</sup> and B3LYP-D3<sup>32</sup> basis sets were used to calculate the single-point energies, which could provide energetic information. The energies given in this work are the relative free energies and enthalpies calculated by M06 and B3LYP-D3 methods in acetonitrile solvent.

**DFT Studies on C–H Activation and Carbene Formation.** The energy profiles (free energy and enthalpy) calculated by DFT methods M06 and B3LYP for the three possible pathways are shown in Figures 1–3, and these two methods offered consistent and thus reliable results, so only the free energy is discussed. Active catalyst **CP1** ( $\text{RhCp}^*(\text{OAc})_2$ ) interacts with phenacyl triethylammonium bromide **1a** to form C-bound enolate **CP2** or its O-bound isomer **CP14** (Figure 1).<sup>33</sup> Enolate complex **CP2** undergoes an acetate-assisted, reversible C–H activation via a concerted transition state **TS1** (the CMD mechanism) with an activation free energy of 27.2 kcal/mol, after which the 16-electron cyclometalated intermediate **CP3** is formed with the release of an acetic acid. The coordination of the diazo substrate to **CP3** forms intermediate **CP4** with 10.0 kcal/mol endothermicity. The subsequent denitrogenation of intermediate **CP4** readily gives **CP5** via transition state **TS2** and carries a kinetic barrier of only 9.5 kcal/mol, and the overall free energy of the **TS2** is 22.9 kcal/mol. Alternatively (pathway A', green lines), the formation of an O-bound enolate intermediate **CP14** is endogonic by 8.7 kcal/mol and the subsequent O-coordination assisted C–H activation occurs via transition state **TS11** which has an overall free energy of 29.5 kcal/mol, and it is 2.5 kcal/mol higher than the C-bound transition state **TS1**. Thus, C–H activation assisted by C-coordination of the enolate has a lower calculated barrier. Following pathway A', coordination of diazo substrate **2a** forms intermediate **CP16**, and the subsequent denitrogenation of **CP16** takes place via transition state **TS12** with an activation free energy of 13.1 kcal/mol to generate carbene species **CP17**. **CP17** then undergoes linkage isomerization to afford the same C-bound intermediate **CP5**. Clearly, pathway A' is kinetically disfavored in terms of both C–H activation and subsequent denitrogenation.

**DFT Studies on Mechanistic Possibilities of C–C Formation.** Following the denitrogenation process, carbene species **CP5** is the common intermediates for all the three plausible pathways. As shown in Figure 2, in pathway A (black lines), Rh–aryl migratory insertion of **CP5** to afford **CP6** via **TS3** is irreversible and occurs with a barrier of 10.2 kcal/mol. Alternatively, it has been proposed that **CP6** might be

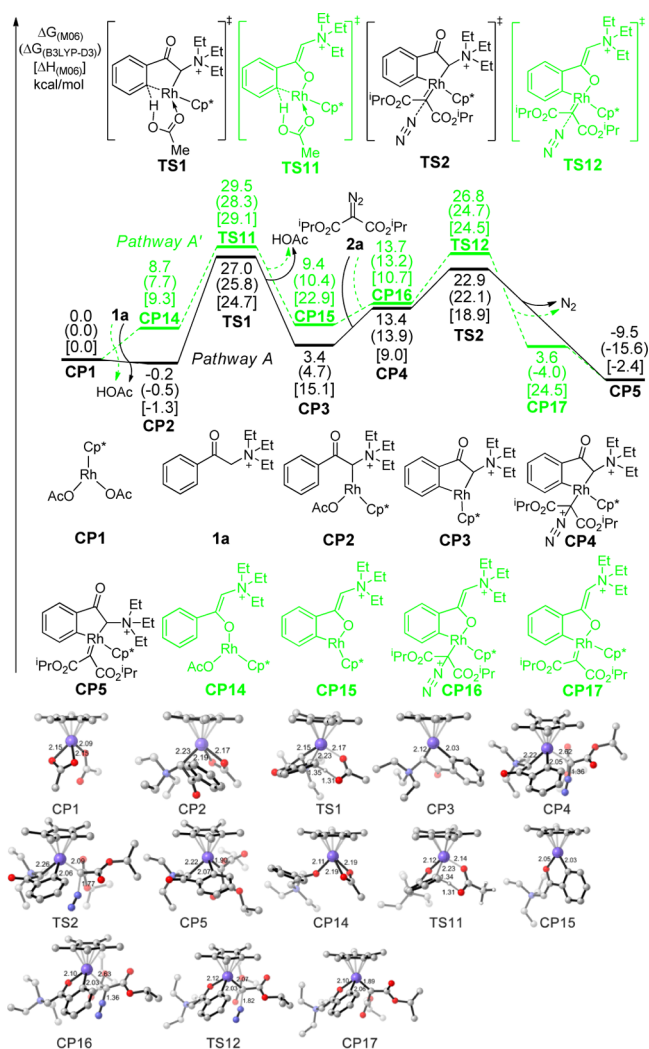


**Figure 1.** Energy profiles and geometry information for the C–H activation and denitrogenation steps. The values given by kcal/mol are the relative free energies calculated by M06 method in acetonitrile solvent. The values in parentheses are the free energies given by B3LYP-D3 method. The values in square brackets are the enthalpies obtained from the M06 method.

generated directly from intermediate **CP4** without any carbene species: the Rh–aryl bond might undergo 1,2-migratory insertion with concomitant displacement of the dinitrogen leaving group.<sup>18</sup> We evaluated this possibility and found that the activation free energy (34.0 kcal/mol) for this elementary step is so high (24.5 kcal/mol higher than the that of carbene-involved pathway) that it is not a reasonable pathway (see SI, Figure S2).

The resulting dialkyl complex **CP6** irreversibly eliminates a triethylamine via **TS4** with the coordination of an acetate to give  $\alpha$ -oxo carbenoid intermediate **CP7** and this elimination holds an overall activation free energy of 25.2 kcal/mol. The second carbene insertion of **CP7** irreversibly generates a Rh enolate intermediate **CP8** via the transition **TSS5** with a strikingly low barrier of 2.1 kcal/mol. This low barrier is likely due to the high reactivity of the rhodium  $\alpha$ -oxo carbenoid species.<sup>27</sup> Protonolysis of intermediate **CP8** eventually affords the final product **3aa** with the regeneration of the catalyst **CP1** with slight exothermicity.

In pathway B (blue lines), the Rh–alkyl bond in **CP5** undergoes migratory insertion to give **CP9** via **TS6**, and the calculated free energy of the transition state **TS6** is 10.8 kcal/mol, which is 10.1 kcal/mol higher than the **TS3**. This indicates that migratory of an alkyl group is slower and is in agreement with various studies. Subsequent C–C

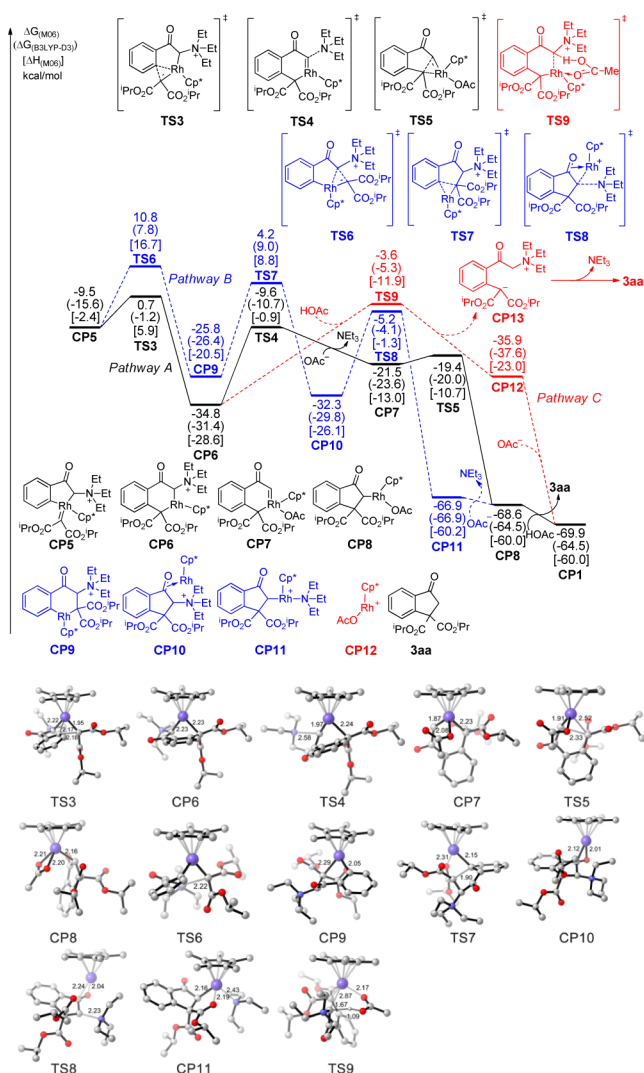


**Figure 2.** Energy profiles and geometric information for the three competitive mechanisms of rhodium-catalyzed activation of phenacyl ammonium salts. The values given by kcal/mol are the relative free energies calculated by the M06 method in acetonitrile solvent. The values in parentheses are the free energies given by the B3LYP-D3 method. The values in square brackets are the enthalpies given by the M06 method.

reductive elimination of **CP9** is calculated to proceed via transition state **TS7** with an activation free energy of 30.0 kcal/mol, affording a Rh(I)  $\pi$ -ketone complex **CP10**. Alternatively, **CP10** can be generated from the direct reductive elimination of **CP6**. However, the calculated activation free energy for this reductive elimination is 37.8 kcal/mol (see SI, Figure S3), so this alternative is unlikely. The polar C–N bond in **CP10** oxidatively adds back to the Rh(I) to irreversibly afford intermediate **CP11** via transition state **TS8** with a calculated barrier of 27.1 kcal/mol. Ligand substitution of **CP11** with an incoming acetate can also generate the common intermediate **CP8**. In comparison with the data in pathway A, the free energy of transition states **TS6** in pathway B is 10.1 kcal/mol higher than that of transition state **TS3**. Therefore, pathway A is favored.

In pathway C (red), the Rh(III)–alkyl intermediate **CP6** is cleaved by acetic acid via transition state **TS9** with an activation free energy of 31.2 kcal/mol, which is 6.0 kcal/mol higher than the **TS4**, to form a cationic rhodium intermediate **CP12** and a zwitterionic intermediate **CP13**, which leads to the regeneration of the catalyst **CP1** upon ligation of an acetate. One molecule of triethylamine is released from intermediate **CP10** via intramolecular  $S_N2$  substitution through

transition state **TS10** (Figure 3) with a barrier of 19.0 kcal/mol. Compared with pathway A, this pathway is also unfavorable (for an alternative but also unlikely protolysis pathway, see SI, Figure S4).

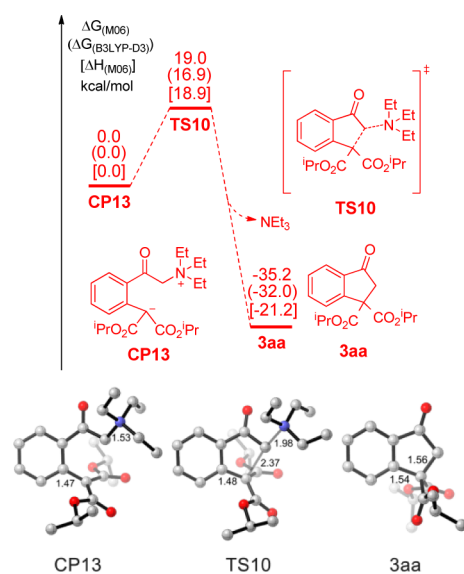


**Figure 3.** Energy profiles and geometric information for the intramolecular  $S_N2$  substitution of the possible intermediate **CP13**. The values given by kcal/mol are the relative free energies calculated by the M06 method in acetonitrile solvent. The values in parentheses are the free energies given by the B3LYP-D3 method. The values in square brackets are the enthalpies given by the M06 method.

As a summary of our theoretical studies, the most likely mechanism for this coupling reaction is outlined in pathway A, which includes sequential steps of C-coordination of the substrate, C–H activation, denitrogenation, carbene insertion,  $\alpha$ -elimination of  $NEt_3$ , a second carbene insertion, and protonolysis. The DFT-established  $\alpha$ -carbenoid species in this lowest energy pathway seems in good agreement with recent theoretical studies on the C–H activation of *N*-pivaloxybenzamide,<sup>34</sup> where a rhodium nitrene species which was regarded as Rh(V) has been established as a key intermediate. Our DFT studies suggest that the C–H activation process is rate-limiting, which agree well with our experimental KIE results. The calculated overall activation free energy of 27.2 kcal/mol is in line with the kinetic profile of an efficient reaction at 80 °C. While there seems to be discrepancy between experimental and theoretical studies on the reversibility of C–H activation, the DFT studies refer to standard conditions with 1 atm HOAc. However, in the real catalytic system with CsOAc, it is likely that the rate of the protonolysis reaction (**CP3**  $\rightarrow$  **CP2**) is significantly slower such that C–H activation is no longer reversible.

## CONCLUSION

We have designed phenacyl triethylammonium salts as novel but readily available arene substrates for redox-neutral couplings with  $\alpha$ -diazo esters and simple olefins via a C–H activation pathway. In these systems, the polar C–N bond acts as an oxidizing directing group to facilitate *ortho* C–H activation. The coupling with  $\alpha$ -diazo esters afforded benzocyclopentanones, and the coupling with olefins furnished *ortho*-olefinated acetophenones. A broad scope of substrates has been established, and the reactions proceeded with high efficiency and with functional group tolerance. Moreover, the coupling of diazo esters can be achieved in one pot starting from  $\alpha$ -bromoacetophenones as a readily available substrate.

The reaction mechanism for the coupling of phenacyl triethylammonium bromides with diazo esters has been explored by a combination of experimental and theoretical methods. In particular, three distinct mechanistic pathways have been scrutinized by DFT studies, which revealed that, in the lowest energy pathway, the C–H activation occurs via a concerted metalation–deprotonation mechanism, with the cyclometalation being assisted by C-coordination rather than O-coordination. The lowest energy pathway also involves two Rh(III) carbene species (and consequently two migratory insertion steps) as key intermediates. The first one is generated via coordination and denitrogenation of a diazo ester, and the second  $\alpha$ -oxo carbene originates from migratory insertion of the Rh–aryl bond into the first carbene, followed by  $\alpha$ -elimination of  $NEt_3$ . The C–H activation process was established to be the rate-limiting step on the basis of DFT and experimental studies. The chemistry of using this rare oxidizing C–N directing group will broaden the scope and applications of rhodium(III)-catalyzed C–H activation, and may find applications in the efficient synthesis of complex structures.

## ASSOCIATED CONTENT

### Supporting Information

Experimental procedures, characterization data, NMR spectra of the products, and DFT data. This material is available free of charge via the Internet at <http://pubs.acs.org>.

## AUTHOR INFORMATION

### Corresponding Authors

\*xwli@dicp.ac.cn

\*lanyu@cqu.edu.cn

\*bswan@dicp.ac.cn

### Notes

The authors declare no competing financial interest.

## ACKNOWLEDGMENTS

This work has been supported by the Dalian Institute of Chemical Physics (Chinese Academy of Sciences), the Key Research Program of the Chinese Academy of Sciences, and the NSFC (Nos. 21272231, 21472186, 21372266, and 51302327). We thank Yimeng Zhang for some initial screenings and Prof. Qilong Shen (SIOC, CAS) for useful discussions.

## REFERENCES

- Reviews on Rh-catalyzed C–H activation: (a) Satoh, T.; Miura, M. *Chem.—Eur. J.* **2010**, *16*, 11212–11222. (b) Wencel-Delord, J.; Droge, T.; Liu, F.; Glorius, F. *Chem. Soc. Rev.* **2011**, *40*, 4740–4761. (c) Song, G.; Wang, F.; Li, X. *Chem. Soc. Rev.* **2012**, *41*, 3651–3678. (d) Colby, D. A.; Bergman, R. G.; Ellman, J. A. *Chem. Rev.* **2010**, *110*, 624–655. (e) Kuhl, N.; Schröder, N.; Glorius, F. *Adv. Synth. Catal.* **2014**, *356*, 1443–1460. Other general reviews on C–H activation: (f) Gutekunst, W. R.; Baran, P. S. *Chem. Soc. Rev.* **2011**, *40*, 1976–1991. (g) McMurray, L.; O'Hara, F.; Gaunt, M. J. *Chem. Soc. Rev.* **2011**, *40*, 1885–1898. (h) Yeung, C. S.; Dong, V. M. *Chem. Rev.* **2011**, *111*, 1215–1292. (i) Sun, C.-L.; Li, B.-J.; Shi, Z.-J. *Chem. Rev.* **2011**, *111*, 1293–1314. (j) White, M. C. *Science* **2012**, *335*, 807–809. (k) Wendlandt, A. E.; Suess, A. M.; Stahl, S. S. *Angew. Chem., Int. Ed.* **2011**, *50*, 11062–11087. (l) Cho, S. H.; Kim, J. Y.; Kwak, J.; Chang, S. *Chem. Soc. Rev.* **2011**, *40*, 5068–5083. (m) Arockiam, P. B.; Bruneau, C.; Dixneuf, P. H. *Chem. Rev.* **2012**, *112*, 5879–5918.
- Selected reviews on heterocycle synthesis through C–H functionalization: (a) Yamaguchi, J.; Yamaguchi, A. D.; Itami, K. *Angew. Chem., Int. Ed.* **2012**, *51*, 8960–9009. (b) Lyons, T. W.;



- Sanford, M. S. *Chem. Rev.* **2010**, *110*, 1147–1169. (c) Chen, X.; Engle, K. M.; Wang, D.-H.; Yu, J.-Q. *Angew. Chem., Int. Ed.* **2009**, *48*, 5094–5115. (d) Seregin, I. V.; Gevorgyan, V. *Chem. Soc. Rev.* **2007**, *36*, 1173–1193. (e) Ackermann, L. *Acc. Chem. Res.* **2014**, *47*, 281–295. (f) Zhang, X.-S.; Chen, K.; Shi, Z.-J. *Chem. Sci.* **2014**, *5*, 2146–2159.
- (3) (a) Song, G.; Chen, D.; Pan, C.-L.; Crabtree, R. H.; Li, X. *J. Org. Chem.* **2010**, *75*, 7487–7490. (b) Su, Y.; Zhao, M.; Han, K.; Song, G.; Li, X. *Org. Lett.* **2010**, *12*, 5462–5465. (c) Jayakumar, J.; Parthasarathy, K.; Cheng, C.-H. *Angew. Chem., Int. Ed.* **2012**, *51*, 197–200. (d) Umeda, N.; Tsurugi, H.; Satoh, T.; Miura, M. *Angew. Chem., Int. Ed.* **2008**, *47*, 4019–4022. (e) Shimizu, M.; Hirano, K.; Satoh, T.; Miura, M. *J. Org. Chem.* **2009**, *74*, 3478–3483.
- (4) (a) Michida, S.; Hirano, K.; Satoh, T.; Miura, M. *J. Org. Chem.* **2009**, *74*, 6295–6298. (b) Patureau, F. W.; Besset, T.; Glorius, F. *Angew. Chem., Int. Ed.* **2011**, *50*, 1064–1067. (c) Liu, B.; Fan, Y.; Gao, Y.; Sun, C.; Xu, C.; Zhu, J. *J. Am. Chem. Soc.* **2013**, *135*, 468–473. (d) Zhen, W.; Wang, F.; Zhao, M.; Du, Z.; Li, X. *Angew. Chem., Int. Ed.* **2012**, *51*, 11819–11823.
- (5) (a) Xie, F.; Qi, Z.; Li, X. *Angew. Chem., Int. Ed.* **2013**, *52*, 11862–11866. (b) Yang, Y.; Hou, W.; Qin, L.; Du, J.; Feng, H.; Zhou, B.; Li, Y. *Chem.—Eur. J.* **2014**, *20*, 416–420.
- (6) (a) Cui, S.; Zhang, Y.; Wu, Q. *Chem. Sci.* **2013**, *4*, 3421–3426. (b) Davis, T. A.; Hyster, T. K.; Rovis, T. *Angew. Chem., Int. Ed.* **2013**, *52*, 5364–5367. (c) Cui, S.; Zhang, Y.; Wang, D.; Wu, Q. *Chem. Sci.* **2013**, *4*, 3912–3916. (d) Zeng, R.; Wu, S.; Fu, C.; Ma, S. *J. Am. Chem. Soc.* **2013**, *135*, 18284–18287. (e) Wang, H.; Glorius, F. *Angew. Chem., Int. Ed.* **2012**, *51*, 7318–7322. (f) Lian, Y.; Huber, T.; Hesp, K. D.; Bergman, R. G.; Ellman, J. A. *Angew. Chem., Int. Ed.* **2013**, *52*, 629–633. (g) Wang, H.; Grohmann, C.; Nimphius, C.; Glorius, F. *J. Am. Chem. Soc.* **2012**, *134*, 19592–19595. (h) Lam, H.-W.; Man, K.-Y.; Chan, W.-W.; Zhou, Z.; Yu, W.-Y. *Org. Biomol. Chem.* **2014**, *12*, 4112–4116. (i) Neely, J. M.; Rovis, T. *J. Am. Chem. Soc.* **2013**, *135*, 66–69. (j) Hytser, T. K.; Ruhl, K. E.; Rovis, T. *J. Am. Chem. Soc.* **2013**, *135*, 5364–5367. (k) Ye, B.; Cramer, N. *Angew. Chem., Int. Ed.* **2014**, *53*, 7896–7899. For a recent review on C–H activation using internal oxidants with N–O cleavage, see: (l) Huang, H.; Ji, X.; Wu, W.; Jiang, H. *Chem. Soc. Rev.* **2015**, DOI: 10.1039/c4cs00288a.
- (7) (a) Guimond, N.; Gorelsky, S. I.; Fagnou, K. *J. Am. Chem. Soc.* **2011**, *133*, 6449–6457. (b) Guimond, N.; Gouliaras, C.; Fagnou, K. *J. Am. Chem. Soc.* **2010**, *132*, 6908–6909.
- (8) (a) Rakshit, S.; Grohmann, C.; Besset, T.; Glorius, F. *J. Am. Chem. Soc.* **2011**, *133*, 2350–2353. (b) Patureau, F. W.; Glorius, F. *Angew. Chem., Int. Ed.* **2011**, *50*, 1977–1979.
- (9) (a) Too, P. C.; Wang, Y.-F.; Chiba, S. *Org. Lett.* **2010**, *12*, 5688–5691. (b) Zhang, X.; Chen, D.; Zhao, M.; Zhao, J.; Jia, A.; Li, X. *Adv. Synth. Catal.* **2011**, *353*, 719–723. (c) Neely, J. M.; Rovis, T. *J. Am. Chem. Soc.* **2013**, *135*, 66–69. (d) Zhou, B.; Hou, W.; Yang, Y.; Li, Y. *Chem.—Eur. J.* **2013**, *19*, 4701–4706. (e) Huckins, J. R.; Bercot, E. A.; Thiel, O. R.; Hwang, T.-L.; Bio, M. M. *J. Am. Chem. Soc.* **2013**, *135*, 14492–14495. (f) Hyster, T. K.; Rovis, T. *Chem. Commun.* **2011**, *47*, 11846–11848.
- (10) (a) Zhao, D.; Shi, Z.; Glorius, F. *Angew. Chem., Int. Ed.* **2013**, *52*, 12426–12429. (b) Chuang, S.-C.; Gandeepan, P.; Cheng, C.-H. *Org. Lett.* **2013**, *15*, 5750–5753. (c) Zheng, L.; Hua, R. *Chem.—Eur. J.* **2014**, *20*, 2352–2356. (d) Liang, Y.; Yu, K.; Li, B.; Xu, S.; Song, H.; Wang, B. *Chem. Commun.* **2014**, *50*, 6130–6133. (e) Han, W.; Zhang, G.; Li, G.; Huang, H. *Org. Lett.* **2014**, *16*, 3532–3535. (f) Muralirajan, K.; Cheng, C.-H. *Adv. Synth. Catal.* **2014**, *356*, 1571–1576.
- (11) (a) Liu, G.; Shen, Y.; Zhou, Z.; Lu, X. *Angew. Chem., Int. Ed.* **2013**, *52*, 6033–6037. (b) Hu, F.; Xia, Y.; Ye, F.; Liu, Z.; Ma, C.; Zhang, Y.; Wang, J. *Angew. Chem., Int. Ed.* **2014**, *53*, 1364–1367. (c) Zhang, H.; Wang, K.; Wang, B.; Yi, H.; Hu, F.; Li, C.; Zhang, Y.; Wang, J. *Angew. Chem., Int. Ed.* **2014**, *53*, 13234–13238. (d) Chen, Y.; Wang, D.; Duan, P.; Ben, R.; Dai, L.; Shao, X.; Hong, M.; Zhao, J.; Huang, Y. *Nat. Commun.* **2014**, *5*, No. 4610. For a Pd-catalyzed coupling of phenoxamides, see: (e) Duan, P.; Yang, Y.; Ben, R.; Yan, Y.; Dai, L.; Hong, M.; Wu, Y.-D.; Wang, D.; Zhang, X.; Zhao, J. *Chem. Sci.* **2014**, *5*, 1574–1578.
- (12) (a) Wu, J.; Cui, X.; Chen, L.; Jiang, G.; Wu, Y. *J. Am. Chem. Soc.* **2009**, *131*, 13888–13889. (b) Huang, X.; Huang, J.; Du, C.; Zhang, X.; Song, F.; You, J. *Angew. Chem., Int. Ed.* **2013**, *52*, 12970–12974. (c) Zhang, X.; Qi, Z.; Li, X. *Angew. Chem., Int. Ed.* **2014**, *53*, 10794–10798.
- (13) (a) Liu, B.; Song, C.; Sun, C.; Zhou, S.; Zhu, J. *J. Am. Chem. Soc.* **2013**, *135*, 16625–16631. (b) Wang, C.; Huang, Y. *Org. Lett.* **2013**, *15*, 5294–5297. (c) Zhang, Q.-R.; Huang, J.-R.; Zhang, W.; Dong, L. *Org. Lett.* **2014**, *16*, 1684–1687. (d) Tan, Y.; Hartwig, J. F. *J. Am. Chem. Soc.* **2010**, *132*, 3676–3677.
- (14) Shi and co-workers described Rh(III)-catalyzed synthesis of indenones from annulations of benzamides with alkynes via C(O)–N bond cleavage. However, this occurs via a substitution mechanism, and the C–N bond does not function as an oxidizing group. See: Li, B.-J.; Wang, H.-Y.; Zhu, Q.-L.; Shi, Z.-J. *Angew. Chem., Int. Ed.* **2012**, *51*, 3948–3952.
- (15) (a) Engle, K. M.; Mei, T.-S.; Wasa, M.; Yu, J.-Q. *Acc. Chem. Res.* **2012**, *45*, 788–802. (b) Kim, J.; Chang, S. *Angew. Chem., Int. Ed.* **2014**, *53*, 2203–2207. (c) Padala, K.; Jeganmohan, M. *Org. Lett.* **2011**, *13*, 6144–6147. (d) Muralirajan, K.; Parthasarathy, K.; Cheng, C.-H. *Angew. Chem., Int. Ed.* **2011**, *50*, 4169–4172. (e) Patureau, F. W.; Besset, T.; Kuhl, N.; Glorius, F. *J. Am. Chem. Soc.* **2011**, *133*, 2154–2156.
- (16) Yu, D.-G.; de Azambuja, F.; Glorius, F. *Angew. Chem., Int. Ed.* **2014**, *53*, 2754–2758.
- (17) (a) Tan, X.; Liu, Bi.; Li, X.; Li, B.; Xu, S.; Song, H.; Wang, B. *J. Am. Chem. Soc.* **2012**, *134*, 16163–16166. For a related Ru(II) system, see: (b) Mehta, V. P.; Garcia-Lopez, J.-A.; Greaney, M. *Angew. Chem., Int. Ed.* **2014**, *53*, 1529–1533. No C( $\alpha$ )–C bond cleavage was involved in these systems.
- (18) For examples of coupling of diazoesters in C–H activation, see: (a) Chan, W.-W.; Lo, S.-F.; Zhou, Z.; Yu, W.-Y. *J. Am. Chem. Soc.* **2012**, *134*, 13565–13568. (b) Yu, X.; Yu, S.; Xiao, J.; Wan, B.; Li, X. *J. Org. Chem.* **2013**, *78*, 5444–5452. (c) Shi, J.; Yan, Y.; Li, Q.; Xu, H. E.; Yi, W. *Chem. Commun.* **2014**, *50*, 6483–6486. (d) Ai, W.; Yang, X.; Wu, Y.; Wang, X.; Li, Y.; Yang, Y.; Zhou, B. *Chem.—Eur. J.* **2014**, *20*, 17653–17657.
- (19) (a) Ren, X.; Wen, P.; Shi, X.; Wang, Y.; Li, J.; Yang, S.; Han, H.; Huang, G. *Org. Lett.* **2013**, *15*, 5194–5197. (b) Wang, F.; Song, G.; Li, X. *Org. Lett.* **2010**, *12*, 5430–5433.
- (20) (a) Li, X.; Yu, S.; Wang, F.; Wan, B.; Yu, X. *Angew. Chem., Int. Ed.* **2013**, *52*, 2577–2580. (b) Xie, F.; Qi, Z.; Yu, S.; Li, X. *J. Am. Chem. Soc.* **2014**, *136*, 4780–4787.
- (21) Imoto, H.; Sugiyama, Y.; Kimura, H.; Momose, Y. *Chem. Pharm. Bull.* **2003**, *51*, 138–151.
- (22) (a) Brea, J.; Rodrigo, J.; Carrieri, A.; Sanz, F.; Cadavid, M. I.; Enguix, M. J.; Villazon, M.; Mengod, G.; Caro, Y.; Masaguer, C. F.; Ravina, E.; Centeno, N. B.; Carotti, A.; Loza, M. I. *J. Med. Chem.* **2002**, *45*, 54–71. (b) Ravina, E.; Negreira, J.; Cid, J.; Masaguer, C. F.; Rosa, E.; Rivas, M. E.; Fontenla, J. A.; Loza, M. I.; Tristan, H.; Cadavid, M. I.; Sanz, F.; Lozoya, E.; Carotti, A.; Carrieri, A. *J. Med. Chem.* **1999**, *42*, 2774–2797.
- (23) (a) Lu, Y.; Wang, D.-H.; Engle, K. M.; Yu, J.-Q. *J. Am. Chem. Soc.* **2010**, *132*, 5916–5921. (b) Tsai, A. S.; Brasse, M.; Bergman, R. G.; Ellman, J. A. *Org. Lett.* **2011**, *13*, 540–542. (c) Wang, Z.; Reinus, B. J.; Dong, G. *J. Am. Chem. Soc.* **2012**, *134*, 13954–13957. (d) Huang, L.; Wang, Q.; Qi, J.; Wu, X.; Huang, K.; Jiang, H. *Chem. Sci.* **2013**, *4*, 2665–2669. (e) Zhang, T.; Qi, Z.; Zhang, X.; Wu, L.; Li, X. *Chem.—Eur. J.* **2014**, *20*, 3283–3287. (f) Zhu, C.; Falck, J. R. *Org. Lett.* **2011**, *13*, 1214–1217. (g) Deb, A.; Bag, S.; Kancheria, R.; Maiti, D. *J. Am. Chem. Soc.* **2014**, *136*, 13602–13605.
- (24) (a) Shen, Y.; Liu, G.; Zhou, Z.; Lu, X. *Org. Lett.* **2013**, *15*, 3366–3369. (b) Li, B.; Ma, J.; Wang, N.; Feng, H.; Xu, S.; Wang, B. *Org. Lett.* **2012**, *14*, 736–739.
- (25) (a) Piou, T.; Rovis, T. *J. Am. Chem. Soc.* **2014**, *136*, 11292–11295. (b) Seoane, A.; Casanova, N.; Quiñones, N.; Mascareñas, J. L.; Gulías, M. *J. Am. Chem. Soc.* **2014**, *136*, 7607–7610.
- (26) (a) Shi, Z.; Koester, D. C.; Boultheadakis-Arapinis, M.; Glorius, F. *J. Am. Chem. Soc.* **2013**, *135*, 12204–12207. (b) Li, X. G.; Sun, M.; Jin,



Q.; Liu, P. N. *Chem. Commun.* **2014**, DOI: 10.1039/c4cc09314c.  
(c) Shi, J.; Zhou, J.; Yan, Y.; Jia, J.; Liu, X.; Song, H.; Xu, H. E.; Yi, W. *Chem. Commun.* **2015**, *51*, 668–671.

(27) For a review on  $\alpha$ -oxo carbenoids in catalysis, see: Xiao, J.; Li, X. *Angew. Chem., Int. Ed.* **2011**, *50*, 7226–7236.

(28) Frisch, M. J.; Trucks, G. W.; Schlegel, H. B.; Scuseria, G. E.; Robb, M. A.; Cheeseman, J. R.; Scalmani, G.; Barone, V.; Mennucci, B.; Petersson, G. A.; Nakatsuji, H.; Caricato, M.; Li, X.; Hratchian, H. P.; Izmaylov, A. F.; Bloino, J.; Zheng, G.; Sonnenberg, J. L.; Hada, M.; Ehara, M.; Toyota, K.; Fukuda, R.; Hasegawa, J.; Ishida, M.; Nakajima, T.; Honda, Y.; Kitao, O.; Nakai, H.; Vreven, T.; Montgomery, J. A.; Peralta, J. E.; Ogliaro, F.; Bearpark, M.; Heyd, J. J.; Brothers, E.; Kudin, K. N.; Staroverov, V. N.; Kobayashi, R.; Normand, J.; Raghavachari, K.; Rendell, A.; Burant, J. C.; Iyengar, S. S.; Tomasi, J.; Cossi, M.; Rega, N.; Millam, J. M.; Klene, M.; Knox, J. E.; Cross, J. B.; Bakken, V.; Adamo, C.; Jaramillo, J.; Gomperts, R.; Stratmann, R. E.; Yazyev, O.; Austin, A. J.; Cammi, R.; Pomelli, C.; Ochterski, J. W.; Martin, R. L.; Morokuma, K.; Zakrzewski, V. G.; Voth, G. A.; Salvador, P.; Dannenberg, J. J.; Dapprich, S.; Daniels, A. D.; Farkas, O.; Foresman, J. B.; Ortiz, J. V.; Cioslowski, J.; Fox, D. J. *Gaussian 09*; Gaussian, Inc.: Wallingford, CT, 2009.

(29) (a) Becke, A. D. *J. Chem. Phys.* **1993**, *98*, 5648–5652. (b) Lee, C.; Yang, W.; Parr, R. G. *Phys. Rev. B* **1988**, *37*, 785–789.

(30) (a) Cancès, E.; Mennucci, B.; Tomasi, J. *J. Chem. Phys.* **1997**, *107*, 3032–3041. (b) Cossi, M.; Barone, V.; Cammi, R.; Tomasi, J. *Chem. Phys. Lett.* **1996**, *255*, 327–335. (c) Barone, V.; Cossi, M.; Tomasi, J. *J. Comput. Chem.* **1998**, *19*, 404–417.

(31) Zhao, Y.; Truhlar, D. G. *Theor. Chem. Acc.* **2008**, *120*, 215–241.

(32) Grimme, S.; Antony, J.; Ehrlich, S.; Krieg, H. *J. Chem. Phys.* **2010**, *132*, 154104-1–154104-19.

(33) In addition to Rh(III) acetate-mediated deprotonation–ligation of the phenacyl ammonium substrate, we also investigated the direct interaction between the  $\alpha$  proton and free  $\text{OAc}^-$ . This deprotonation occurs with 13.7 kcal/mol endothermicity, owing to the high acidity of the substrate (see SI, Figure S1). The resulting enolate can coordinate to CP1 to afford the same CP2 with loss of acetate, so this pathway remains possible.

(34) Xu, L.; Zhu, Q.; Cheng, B.; Xia, Y. *J. Org. Chem.* **2012**, *77*, 3017–3024.